Biochemistry Research using ImageStream Cytometry

The ImageStream system combines high-speed image capture with image quantification to create a statistically powerful microscopy platform, enabling robust discrimination of cells based on their appearance. This document highlights applications of ImageStream cytometry to the field of biochemistry as described in publications, posters and podium presentations. For more information, check out the website: (https://www.amnis.com/biochemistry.html)
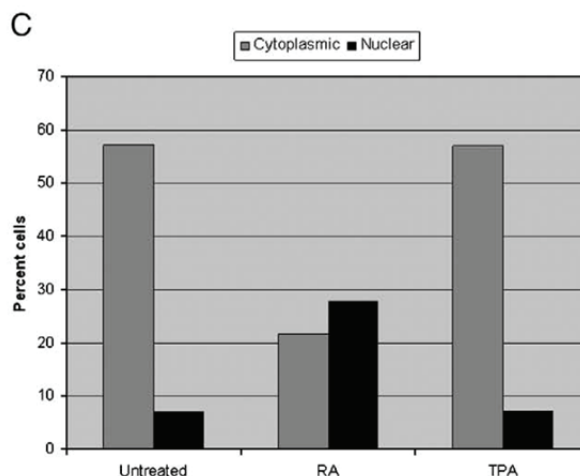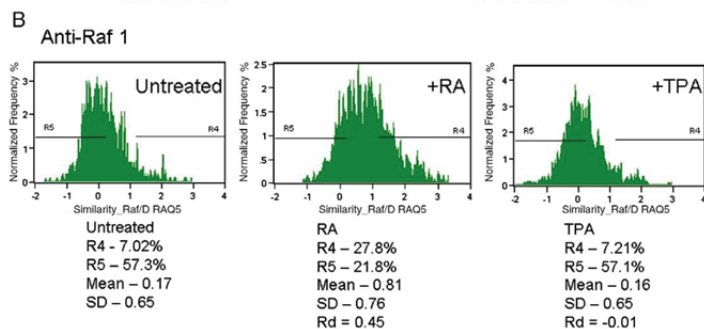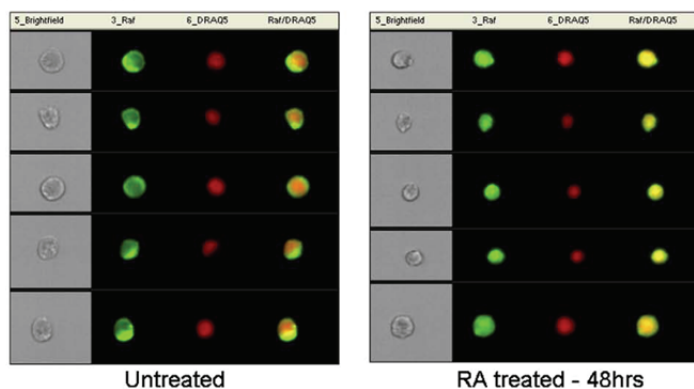
Table of Contents:

RA-induced nuclear translocation of Raf in myelomonocytic leukemia cells

Summary: This ImageStream assay measures Raf1 nuclear localization (by quantifying the similarity between the Raf and nuclear images on a per-cell basis) in HL60 cells differentiating in retinoic acid (RA) or tissue plasminogen activator (TPA) spiked media.

"Differentiating cells in RA induces a quantifiable increase in Raf1 nuclear localization (Rd 0.45). By contrast TPA, which is a known activator of Raf, fails to cause nuclear localization (Rd −0.01), suggesting a novel regulatory mechanism for Raf1 during RA-induced differentiation."

Reference: Smith, J., R.P. Bunaciu, G. Reiterer, D. Coder, T. George, M. Asaly, and A. Yen, *Retinoic acid induces nuclear accumulation of Raf1 during differentiation of HL-60 cells.* Exp Cell Res, 2009.

~ ~ ~ ~ ~ ~

β-catenin nuclear localization in CD34+ AML cells

Summary: This ImageStream assay measures β-catenin nuclear localization (by quantifying the similarity between the β-catenin and nuclear images on a per-cell basis) in samples derived from patients with AML.
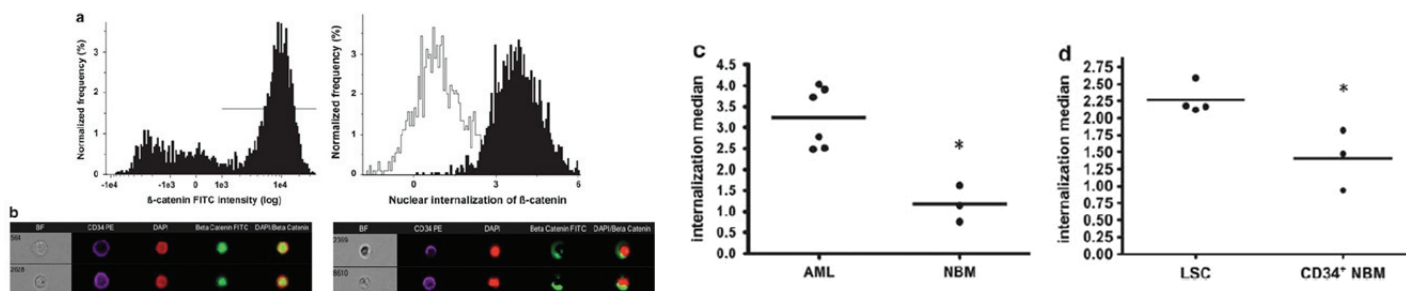
"We further confirmed that the Wnt/b-catenin was actually activated, by determining the degree of b-catenin nuclear residency in AML samples overexpressing b-catenin, using the ImageStream system (Figure 2 and Supplementary Figure S2). Using this approach, we observed that proportionally b-catenin was significantly more localized in the nucleus of CD34þ cells from all AML patients tested compared with those from NBM (Figure 2c), clearly reflecting an increase activation of the Wnt pathway… Once again, we were able to

record that significantly more b-catenin was localized in the nucleus of the LSCs compared with that of CD34þ NBM cells (Figure 2d). Collectively, these data support the conclusion that in most but not all AML samples, Wnt/bcatenin is over-activated and that this is a feature shared by LSCs regardless of their CD34 status..”

Reference: Gandillet, A., S. Park, F. Lassailly, E. Griessinger, J. Vargaftig, A. Filby, T.A. Lister, and D. Bonnet, *Heterogeneous sensitivity of human acute myeloid leukemia to beta-catenin down-modulation.* Leukemia, 2011.

~ ~ ~ ~ ~ ~

Ofatumamab-mediated complement fixation

Summary: This ImageStream assay measures co-localization of C1q to therapeutic antibody on the surface of B cell tumor cells, indicating that Ofatumamab (OFA) mediates complement fixation. This conclusion is made possible because the ImageStream a) rapidly collects thousands of images per sample for good statistics and b) objective quantifies co-localization on a per-cell basis using the bright detail similarity score.
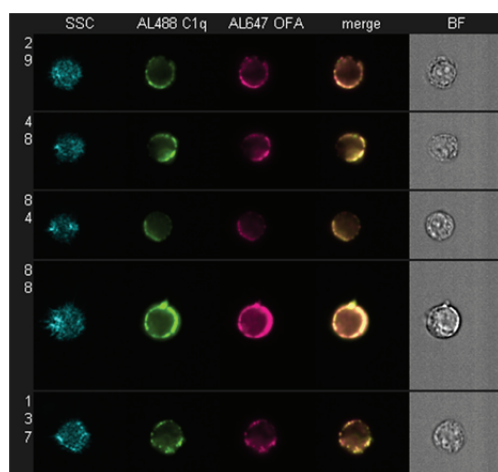

Table I. *Binding of Al488-labeled C1q to mAb-opsonized Daudi cells and colocalization of C1q with mAb*

	Expt. 1			Expt. 2			Expt. 3[a]		
	Al647 mAb (GMF)	Al488 C1q (GMF)	BDSS	Al647 mAb (GMF)	Al488 C1q (GMF)	BDSS	Al647 mAb (GMF)	Al488 C1q (GMF)	BDSS
Al647 OFA	181,000	162,000	3.0	116,000	113,000	3.4	206,000	30,000	2.5
Al647 RTX	186,000	7,500	0.9	61,000	6,600	2.1	155,000	2,200	1.0
Al647 7D8[b]	133,000	2,300	0.6	104,000	1,000	0.9	210,000	1,300	0.7

[a] Different Al488 C1q preparation.
[b] IgG4 (K322A).
BDSS, Bright detail similarity score; GMF, geometric mean fluorescence.

“To test for colocalization quantitatively, double-positive cells (Fig. 2C) were analyzed for colocalization based on an algorithm that calculates the bright detail similarity score. Values of 3–3.5 indicate substantial colocalization, and values of 2.5–3 indicate moderate colocalization. The results of three independent experiments (Table I) reveal that Al488 C1q bound to Al647 OFA-opsonized cells is indeed colocalized with bound OFA.”

Reference: Pawluczkowycz, A.W., F.J. Beurskens, P.V. Beum, M.A. Lindorfer, J.G. van de Winkel, P.W. Parren, and R.P. Taylor, *Binding of submaximal C1q promotes complement-dependent cytotoxicity (CDC) of B cells opsonized with anti-CD20 mAbs ofatumumab (OFA) or rituximab (RTX): considerably higher levels of CDC are induced by OFA than by RTX.* J Immunol, 2009. **183**(1): p. 749-58.

Endosomal trafficking of SLE immune complexes in human monocytes

Summary: This ImageStream assay quantifies the C1q-induced subcellular trafficking of systemic lupus erythematosis (SLE) immune complexes (IC) within human monocytes. The ImageStream's high speed imaging capacity enabled analysis of 10,000 events per sample for robust statistics. The co-localization feature used (bright detail similarity) measures the pixel-by-pixel correlation between the SLE IC and CD71 (or LAMP-1) images.
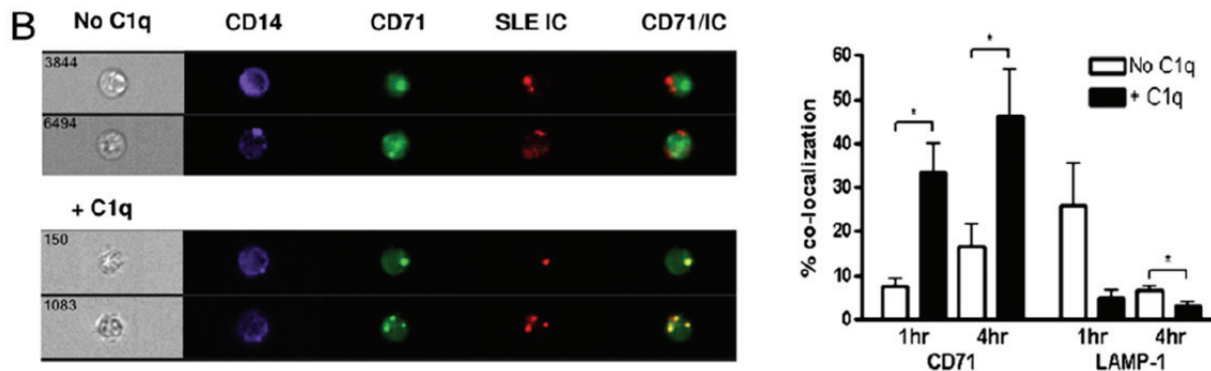
"Our study provides novel evidence to explain how C1q blocks IFN-α production. It demonstrates that C1q enhances the binding of ICs to both monocytes and pDCs. When monocytes were absent, C1q augmented IC binding to pDCs and led to increased IFN-α production. However, when monocytes were present, C1q preferentially and almost exclusively promoted the uptake of ICs by these cells, leading to accumulation in early endosomes and decreased IFN-α production by pDCs."

Reference: Santer, D.M., B.E. Hall, T.C. George, S. Tangsombatvisit, C.L. Liu, P.D. Arkwright, and K.B. Elkon, *C1q deficiency leads to the defective suppression of IFN-alpha in response to nucleoprotein containing immune complexes.* J Immunol, 2010. **185**(8): 4738-49.

~ ~ ~ ~ ~ ~

Quantification of SIRT3 mitochondrial targeting

Summary: This ImageStream assay quantifies the mitochondrial localization of SIRT3-L in H9c2 cells.   Cells were transfected with GFP-N3 (negative control, blue histogram, left images) or GFP-mSIRT3 (red histogram, right images), stained with Mitotracker deep red 633 (red images) and analyzed for co-localization using the Bright Detail similarity score.

"To functionally prove that this novel amino-terminus of mSIRT3-L is a legitimate MLS, we generated a chimera incorporating this cDNA fragment upstream of the reporter gene, GFP (5$_0$-mSirt3- EGFP-N3), and employed ImageStream cytometry for GFP subcellular localization. EGFP-N3 transfected H9c2 cells diffusely expressed GFP with <1% mitochondrial localization. In contrast, 5$_0$- mSirt3-EGFP-N3 expression shows >80% mitochondrial localization (Fig. 1C)."

Reference: Bao, J., Z. Lu, J.J. Joseph, D. Carabenciov, C.C. Dimond, L. Pang, L. Samsel, J.P. McCoy, Jr.*, et al., Characterization of the murine SIRT3 mitochondrial localization sequence and comparison of mitochondrial enrichment and deacetylase activity of long and short SIRT3 isoforms.* J Cell Biochem, 2010. **110**(1): 238-47.
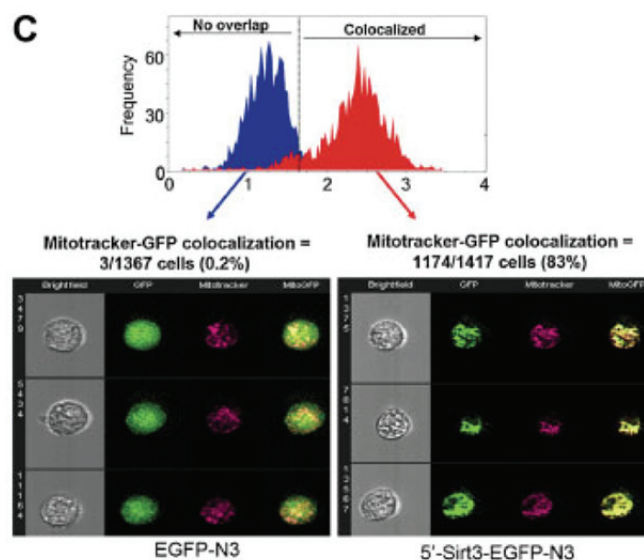
Simultaneous measurement of apoptosis and Noxa mitochondrial localization in HL-60 cells

Summary: This ImageStream assay simultaneously a) discriminates single cells from doublets (left plot, doublets have low aspect ratios), b) discriminates apoptotic from intact cells (center plot: apoptotic cells have reduced nuclear area and increased nuclear texture) and c) measure subcellular localization of 2B3 pS_{12}Noxa (right plot, Similarity quantifies co-localization to mitochondria (MTR)) in HL-60 cells differentiating in retinoic acid (RA) or tissue plasminogen activator (TPA) spiked media.
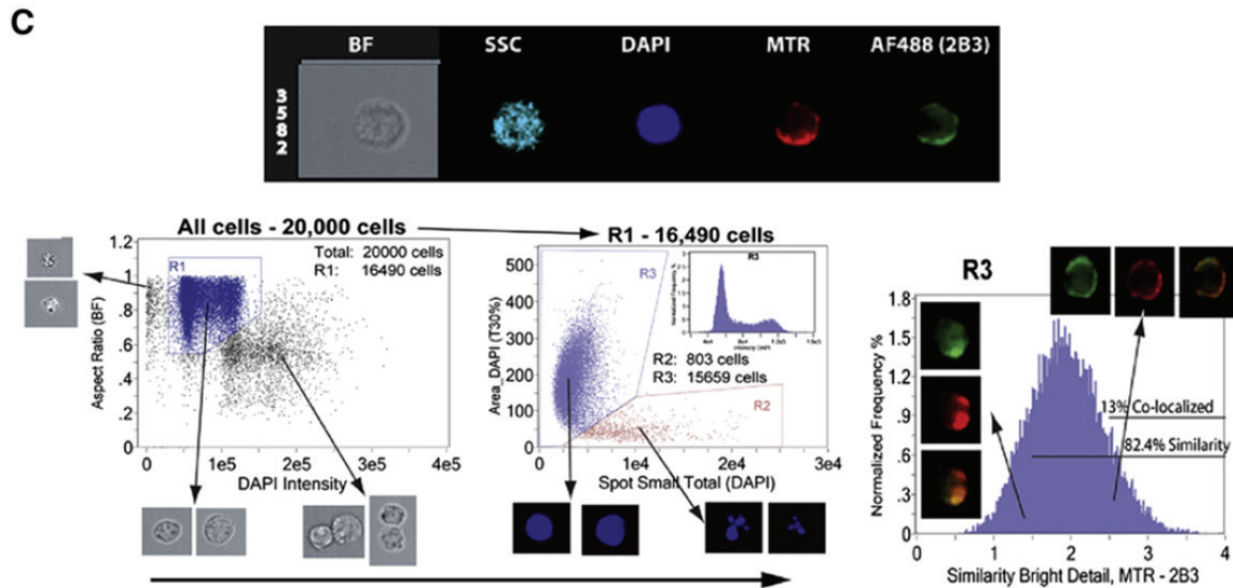
"The ImageStream Multispectral Imaging Flow Cytometer (MIFC), which allows quantification of fluorescence intensity as well as measurement of fluorescent signal distribution and numerous morphological and absorbance characteristics of each cell (Figure 2C), confirmed the cytosolic localization of the pS13Noxa. We were also able to determine that although 82% of pS13 Noxa was in the same (cytosolic and nonnuclear) compartment as mitochondria, only 13% directly colocalized with these organelles."

Reference: Lowman, X.H., M.A. McDonnell, A. Kosloske, O.A. Odumade, C. Jenness, C.B. Karim, R. Jemmerson, and A. Kelekar, *The proapoptotic function of Noxa in human leukemia cells is regulated by the kinase Cdk5 and by glucose.* Mol Cell, 2010. **40**(5): 823-33.

Influenza-induced autophagy and apoptosis in mouse embryonic fibroblasts

Summary: This ImageStream assay simultaneously quantifies autophagy and apoptosis on a per-cell basis in mouse embryonic fibroblasts (MEFs) exposed to UV-B radiation or viral infection. As shown in the plots in (A) and the representative images in (C) and (D), apoptotic cells (R1-green) have high cleaved caspase3 intensity while autophagic cells (R2-red) have high LC3 texture (measured with bright detail intensity). Double positive cells (R3-blue) from the flu-treated sample are also shown in (C).
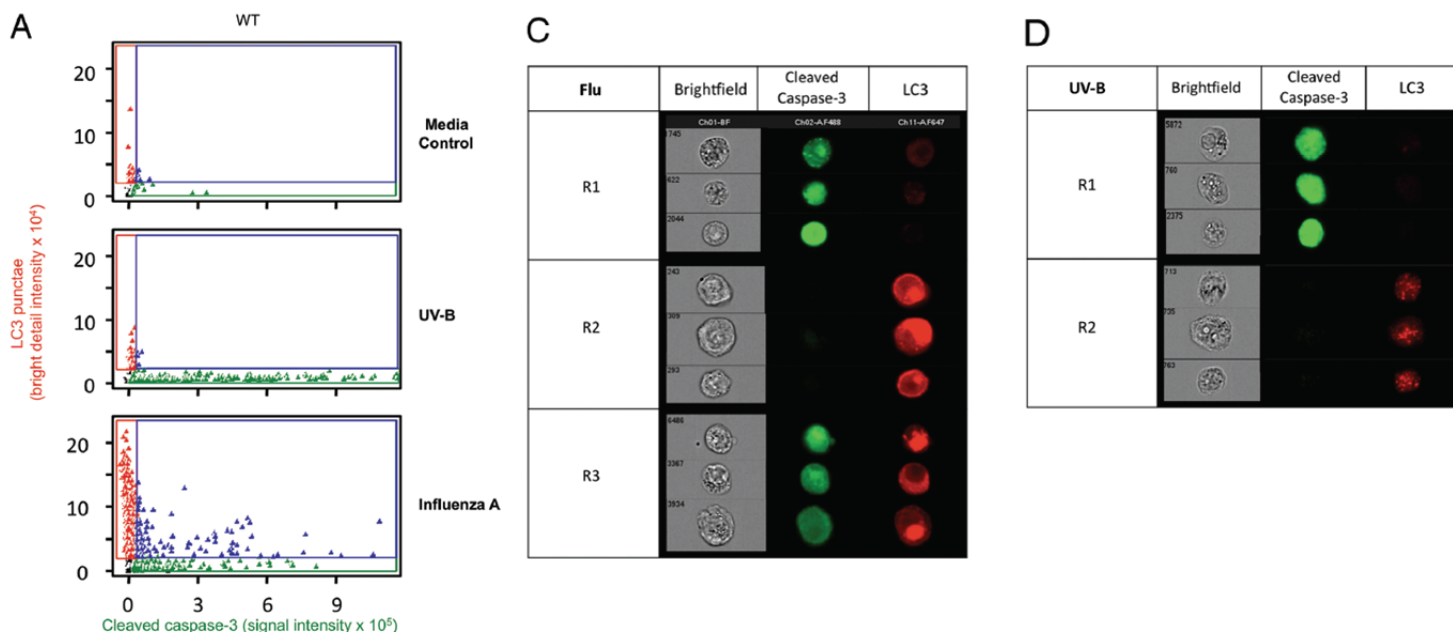
"Multiple stress pathways result in the induction of autophagy and apoptosis. Current methods (e.g., protein gel blot, microscopy) do not offer quantitative single-cell resolution, thus making it difficult to discern if these pathways are mutually exclusive or, in some situations, cooperative in executing cell death. We report a novel method that enables high throughput, high-content assessment of LC3 puncta and caspase-3 cleavage at the single cell level."

Reference: de la Calle, C., Joubert, P., Law, H.K.W., Hasan, M., and M.L. Albert, *Simultaneous assessment of autophagy and apoptosis using multispectral imaging cytometry.* Autophagy, 2011. **7**(9): p. 1-7.

~ ~ ~ ~ ~ ~

uPAR-induced phagocytosis of apoptotic tumor cell fragments

Summary: This ImageStream assay measures the binding and internalization of apoptotic T cell tumor fragments (PKH26) by CS-1 phagocytic cells (GFP+) transfected with Urokinase Plasminogen Activator Receptor (uPAR), β5 integrin, or mock (pCx). Internalization is uniquely measured by quantifying the intensity of the apoptotic material specifically within the internal compartment of the CS-1 cells.

6
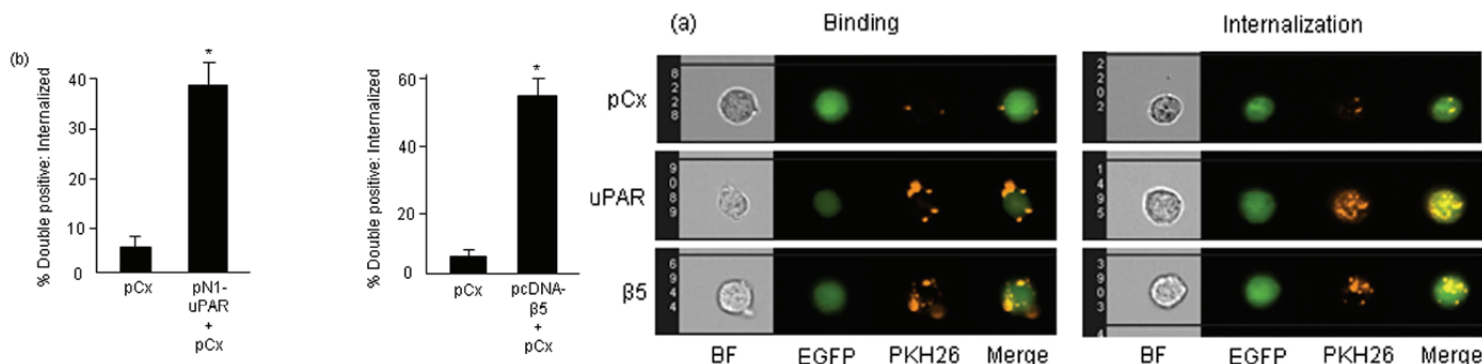
"In the present study, we report that uPAR has a dominant role in the efferocytosis of apoptotic cells, promoting engulfment of apoptotic corpses in transiently overexpressing model phagocytes as well as in breast cancer lines that acquire increased expression of uPAR by epigenetic changes. Because uPAR and the plasminogen activator system are often overexpressed in malignant epithelial carcinomas that include breast, prostate, colon, brain, and others, these data imply that uPAR might confer a phagocytic advantage of uPAR-expressing tumor cells in the tumor microenvironment."

<u>Reference</u>: D'Mello, V., S. Singh, Y. Wu, and R.B. Birge, *The urokinase plasminogen activator receptor promotes efferocytosis of apoptotic cells.* J Biol Chem, 2009. **284**(25): p. 17030-8.

~ ~ ~ ~ ~ ~

Granzyme B content in CD8+ cells from γ chain-deficient mice

<u>Summary</u>: **This ImageStream assay measures granzyme B (GrzB) content (by quantifying the number of granzyme B spots on a per-cell basis) in CD8+ cells from TCR transgenic Bcl2 mice with (P14 Bcl2) or without the common γ chain (P14 Bcl2 γc⁻/⁻) mice.**
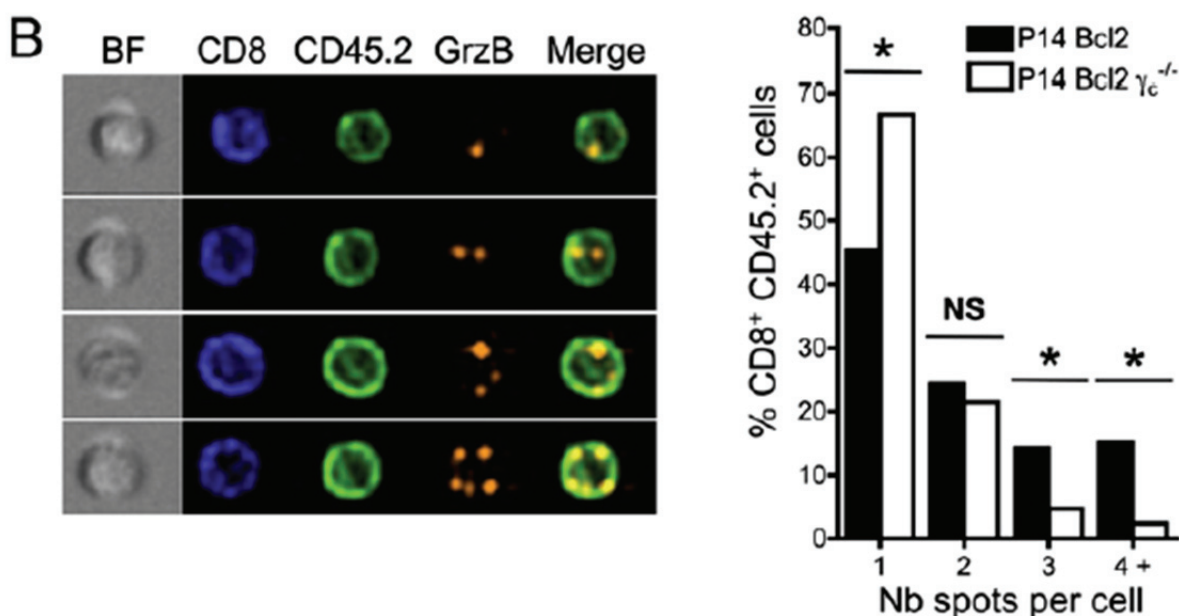
"Morphology and enumeration of granzyme B (GrzB) spots in CD8+ CD45.2+ cells at day 7 postinfection by multispectral imaging. (Left) Representative images showing cells containing 1, 2, 3, and >4 GrzB spots per cell [bright field (BF), CD8, CD45.2, GrzB and composite of CD45.2 and GrzB (merge)]. (Right) Bar graph showing the average distribution of spot counts (mean ± SEM) in P14 Bcl2 (black bars) and P14 Bcl2 γc⁻/⁻ (white bars) CD8+ T cells."

<u>Reference</u>: Decaluwe, H., M. Taillardet, E. Corcuff, I. Munitic, H.K. Law, B. Rocha, Y. Riviere, and J.P. Di Santo, *{gamma}c deficiency precludes CD8+ T cell memory despite formation of potent T cell effectors.* Proc Natl Acad Sci U S A, 2010.

Reference list – Biochemistry applications for the ImageStream

Bao, J., Z. Lu, J.J. Joseph, D. Carabenciov, C.C. Dimond, L. Pang, L. Samsel, J.P. McCoy, Jr., *et al.*, *Characterization of the murine SIRT3 mitochondrial localization sequence and comparison of mitochondrial enrichment and deacetylase activity of long and short SIRT3 isoforms.* J Cell Biochem, 2010. **110**(1): 238-47.

Beum, P.V., M.A. Lindorfer, B.E. Hall, T.C. George, K. Frost, P.J. Morrissey, and R.P. Taylor, *Quantitative analysis of protein co-localization on B cells opsonized with rituximab and complement using the ImageStream multispectral imaging flow cytometer.* J Immunol Methods, 2006. **317**(1-2): 90-9.

Calzada-Nova, G., W.M. Schnitzlein, R.J. Husmann, and F.A. Zuckermann, *North American porcine reproductive and respiratory syndrome viruses inhibit type I interferon production by plasmacytoid dendritic cells.* J Virol, 2011. **85**(6): 2703-13.

Chang, S., K. Kodys, and G. Szabo, *Impaired expression and function of toll-like receptor 7 in hepatitis C virus infection in human hepatoma cells.* Hepatology, 2010. **51**(1): 35-42.

Collins, C.B., J. Ho, T.E. Wilson, J.D. Wermers, J.L. Tlaxca, M.B. Lawrence, M. Solga, J. Lannigan, *et al.*, *CD44 deficiency attenuates chronic murine ileitis.* Gastroenterology, 2008. **135**(6): 1993-2002.

Danis, B., T.C. George, S. Goriely, B. Dutta, J. Renneson, L. Gatto, P. Fitzgerald-Bocarsly, A. Marchant, *et al.*, *Interferon regulatory factor 7-mediated responses are defective in cord blood plasmacytoid dendritic cells.* Eur J Immunol, 2008. **38**(2): 507-17.

de la Calle, C., Joubert, P., Law, H.K.W., Hasan, M., and M.L. Albert, *Simultaneous assessment of autophagy and apoptosis using multispectral imaging cytometry.* Autophagy, 2011. **7**(9): p. 1-7.

Decaluwe, H., M. Taillardet, E. Corcuff, I. Munitic, H.K. Law, B. Rocha, Y. Riviere, and J.P. Di Santo, *Gamma(c) deficiency precludes CD8+ T cell memory despite formation of potent T cell effectors.* Proc Natl Acad Sci U S A, 2010. **107**(20): 9311-6.

D'Mello, V., S. Singh, Y. Wu, and R.B. Birge, *The urokinase plasminogen activator receptor promotes efferocytosis of apoptotic cells.* J Biol Chem, 2009. **284**(25): 17030-8.

Fanning, S.L., T.C. George, D. Feng, S.B. Feldman, N.J. Megjugorac, A.G. Izaguirre, and P. Fitzgerald-Bocarsly, *Receptor cross-linking on human plasmacytoid dendritic cells leads to the regulation of IFN-alpha production.* J Immunol, 2006. **177**(9): 5829-39.

Gandillet, A., S. Park, F. Lassailly, E. Griessinger, J. Vargaftig, A. Filby, T.A. Lister, and D. Bonnet, *Heterogeneous sensitivity of human acute myeloid leukemia to beta-catenin down-modulation.* Leukemia, 2011. **25**(5): 770-80.

George, T.C., S.L. Fanning, P. Fitzgeral-Bocarsly, R.B. Medeiros, S. Highfill, Y. Shimizu, B.E. Hall, K. Frost, *et al.*, *Quantitative measurement of nuclear translocation events using similarity analysis of multispectral cellular images obtained in flow.* J Immunol Methods, 2006. **311**(1-2): 117-29.

Gilcrease, M.Z., X. Zhou, X. Lu, W.A. Woodward, B.E. Hall, and P.J. Morrissey, *Alpha6beta4 integrin crosslinking induces EGFR clustering and promotes EGF-mediated Rho activation in breast cancer.* J Exp Clin Cancer Res, 2009. **28**: 67.

Gruber, F., H. Mayer, B. Lengauer, V. Mlitz, J.M. Sanders, A. Kadl, M. Bilban, R. de Martin, *et al.*, *NF-E2-related factor 2 regulates the stress response to UVA-1-oxidized phospholipids in skin cells.* Faseb J, 2010. **24**(1): 39-48.

Lepelley, A., S. Louis, M. Sourisseau, H.K. Law, J. Pothlichet, C. Schilte, L. Chaperot, J. Plumas, *et al.*, *Innate Sensing of HIV-Infected Cells.* PLoS Pathog, 2011. **7**(2): e1001284.

Lowman, X.H., M.A. McDonnell, A. Kosloske, O.A. Odumade, C. Jenness, C.B. Karim, R. Jemmerson, and A. Kelekar, *The proapoptotic function of Noxa in human leukemia cells is regulated by the kinase Cdk5 and by glucose.* Mol Cell, 2010. **40**(5): 823-33.

Maguire, O., C. Collins, K. O'Loughlin, J. Miecznikowski, and H. Minderman, *Quantifying nuclear p65 as a parameter for NF-kappaB activation: Correlation between ImageStream cytometry, microscopy, and Western blot.* Cytometry A, 2011. **79**(6): 461-9.

Matsuda, J.L., T.C. George, J. Hagman, and L. Gapin, *Temporal dissection of T-bet functions.* J Immunol, 2007. **178**(6): 3457-65.

Megjugorac, N.J., E.S. Jacobs, A.G. Izaguirre, T.C. George, G. Gupta, and P. Fitzgerald-Bocarsly, *Image-based study of interferongenic interactions between plasmacytoid dendritic cells and HSV-infected monocyte-derived dendritic cells.* Immunol Invest, 2007. **36**(5-6): 739-61.

Migueles, S.A., C.M. Osborne, C. Royce, A.A. Compton, R.P. Joshi, K.A. Weeks, J.E. Rood, A.M. Berkley, *et al.*, *Lytic granule loading of CD8+ T cells is required for HIV-infected cell elimination associated with immune control.* Immunity, 2008. **29**(6): 1009-21.

Pawluczkowycz, A.W., F.J. Beurskens, P.V. Beum, M.A. Lindorfer, J.G. van de Winkel, P.W. Parren, and R.P. Taylor, *Binding of submaximal C1q promotes complement-dependent cytotoxicity (CDC) of B cells opsonized with anti-CD20 mAbs ofatumumab (OFA) or rituximab (RTX): considerably higher levels of CDC are induced by OFA than by RTX.* J Immunol, 2009. **183**(1): 749-58.

Raemer, P.C., K. Kohl, and C. Watzl, *Statins inhibit NK-cell cytotoxicity by interfering with LFA-1-mediated conjugate formation.* Eur J Immunol, 2009. **39**(6): 1456-65.

Ramos, H.J., A.M. Davis, T.C. George, and J.D. Farrar, *IFN-alpha is not sufficient to drive Th1 development due to lack of stable T-bet expression.* J Immunol, 2007. **179**(6): 3792-803.

Riddell, J.R., X.Y. Wang, H. Minderman, and S.O. Gollnick, *Peroxiredoxin 1 stimulates secretion of proinflammatory cytokines by binding to TLR4.* J Immunol, 2010. **184**(2): 1022-30.

Rieger, A.M., B.E. Hall, and D.R. Barreda, *Macrophage activation differentially modulates particle binding, phagocytosis and downstream antimicrobial mechanisms.* Dev Comp Immunol, 2010. **34**(11): 1144-59.

Rieger, A.M., B.E. Hall, T. Luong le, L.M. Schang, and D.R. Barreda, *Conventional apoptosis assays using propidium iodide generate a significant number of false positives that prevent accurate assessment of cell death.* J Immunol Methods, 2010. **358**(1-2): 81-92.

Sharma, P.K., R. Singh, K.R. Novakovic, J.W. Eaton, W.E. Grizzle, and S. Singh, *CCR9 mediates PI3K/AKT-dependent antiapoptotic signals in prostate cancer cells and inhibition of CCR9-CCL25 interaction enhances the cytotoxic effects of etoposide.* Int J Cancer, 2010. **127**(9): 2020-30.

Shoshan-Barmatz, V., N. Keinan, S. Abu-Hamad, D. Tyomkin, and L. Aram, *Apoptosis is regulated by the VDAC1 N-terminal region and by VDAC oligomerization: release of cytochrome c, AIF and Smac/Diablo.* Biochim Biophys Acta, 2010. **1797**(6-7): 1281-1291.

Singh, S., R. Singh, U.P. Singh, S.N. Rai, K.R. Novakovic, L.W. Chung, P.J. Didier, W.E. Grizzle, *et al.*, *Clinical and biological significance of CXCR5 expressed by prostate cancer specimens and cell lines.* Int J Cancer, 2009. **125**(10): 2288-95.

Smith, J., R.P. Bunaciu, G. Reiterer, D. Coder, T. George, M. Asaly, and A. Yen, *Retinoic acid induces nuclear accumulation of Raf1 during differentiation of HL-60 cells.* Exp Cell Res, 2009. **315**(13): 2241-8.

Tibrewal, N., Y. Wu, V. D'Mello, R. Akakura, T.C. George, B. Varnum, and R.B. Birge, *Autophosphorylation docking site Tyr-867 in Mer receptor tyrosine kinase allows for dissociation of multiple signaling pathways for phagocytosis of apoptotic cells and down-modulation of lipopolysaccharide-inducible NF-kappaB transcriptional activation.* J Biol Chem, 2008. **283**(6): 3618-27.

Wabnitz, G.H., C. Goursot, B. Jahraus, H. Kirchgessner, A. Hellwig, M. Klemke, M.H. Konstandin, and Y. Samstag, *Mitochondrial translocation of oxidized cofilin induces caspase-independent necrotic-like programmed cell death of T cells.* Cell Death Dis, 2010. **1**(7): e58.

Wang, H., B. Grzywacz, D. Sukovich, V. McCullar, Q. Cao, A.B. Lee, B.R. Blazar, D.N. Cornfield, *et al.*, *The unexpected effect of cyclosporin A on CD56+CD16- and CD56+CD16+ natural killer cell subpopulations.* Blood, 2007. **110**(5): 1530-9.

Yu, D., C.O. Dos Santos, G. Zhao, J. Jiang, J.D. Amigo, E. Khandros, L.C. Dore, Y. Yao, *et al.*, *miR-451 protects against erythroid oxidant stress by repressing 14-3-3{zeta}.* Genes Dev, 2010. **24**(15): 1620-33.